Surface segregation and ordering in III-V semiconductor alloys

Sverre Froyen and Alex Zunger
National Renewable Energy Laboratory, Golden, Colorado 80401
~Received 7 November 1995!

Using the first-principles total-energy pseudopotential method, we have studied the formation energy of the ~001! $Ga_{1-x}In_xP$ alloy surface as a function of composition and reconstruction. The results are presented as $T=0$ surface stability diagrams that show the lowest energy reconstruction and cation occupation pattern as functions of the chemical potentials. Slightly different stability diagrams emanate depending on whether or not there is equilibrium between the surface and the bulk. The stability diagrams show a pronounced asymmetry between the Ga- and In-rich regions. The asymmetry is interpreted in terms of the size difference between In and Ga and the effect of this size difference on the bonding geometry. For surfaces in equilibrium with the bulk, we find a strong dependence of surface segregation on the surface reconstruction, and we predict a Ga enrichment of the surface in the moderate cation-rich limit and In enrichment in the anion-rich region. This result suggests a way to achieve abrupt interfaces in semiconductor heterostructures. For surfaces not in equilibrium with the bulk, we identify regions in the stability diagram where surface-induced CuPt ordering ~both type *A* and type *B*! occurs.

I. INTRODUCTION

The structure of ~001! III-V semiconductor surfaces is strongly dependent on the cation/anion ratio at the surface. For example, the ~001! GaAs surface is observed to form a sequence of different reconstructions ranging from the $c(4\times4)$! and the (2×4)! As-rich to the (4×2)!/$c(8\times2)$! and the (4×6)! Ga-rich surfaces.[1,2] Each reconstruction can be understood as an attempt by the surface to accommodate its valence electrons either in Ga-As, As-As, or Ga-Ga bonding orbitals or in As dangling-bond orbitals. ~001! surfaces of other III-V materials are less well studied but appear to show reconstructions similar to those of GaAs.[3,4] For semiconductor *alloy* surfaces, in addition to the cation/anion ratio, the concentration of the alloying elements must be considered. The combination of surface reconstruction and surface alloying leads to two new features absent from the surfaces of binary zinc-blende semiconductors: surface segregation and surface-induced atomic ordering.

By surface segregation of a given element, we mean enrichment of that element at a surface with respect to the bulk composition. Surface segregation has been extensively studied in metal alloys[5] where thermodynamic equilibrium is easily attained and where the impact of segregation at grain boundaries on metal strength was recognized early. Over the past 10 years, surface segregation studies have also been performed for semiconductor alloys,

pletely understood, or have unit cells too large for our computational resources and will not be considered here. We also avoid the sometimes observed ~2 3 1! and ~1 3 2! reconstructions. Simple dimerized surfaces such as these do not satisfy the so-called electron counting rule[16] that characterizes low-energy surface structures. The electron counting rule simply states that under conditions of charge neutrality, the surface favors a semiconducting structure where all anion dangling bonds are filled and all cation dangling bonds are empty. We nevertheless include the ~2 3 2! reconstruction, which is a modification of the ~1 3 2! surface. This ~2 3 2! recovers its semiconducting properties by making half of the cation dimers asymmetric.[12] For most of the reconstructions discussed above, we study the alloy formation in the top four atomic layers.

The resulting $T = 0$ surface stability diagram is constructed from the $T = 0$ formation energies versus chemical potentials. It provides detailed predictions of surface reconstruction patterns that are stable on the $Ga_{1-x}In_xP$~001! alloy surface. Starting with the cation-rich surfaces, we find that the size difference between Ga and In leads to dramatic differences in the properties of the alloy surface relative to the GaAs~001! surface. The cation-terminated $b2$~4 3 2! reconstruction dominates the Ga-rich region of the alloy surface stability diagram. This reconstruction is also observed for Ga-rich GaAs surfaces. The $b2$~4 3 2! reconstruction is unstable, however, with respect to the anion-terminated $b2$~2 3 4! and cation-terminated

value for the CuPt-chalcopyrite energy difference is in good agreement with the value 28.6 meV per atom from a recent calculation by Lu *et al.*[24] and the chalcopyrite formation energies, 7.8 and 215.0 meV per atom with respect to incoherent and epitaxially coherent ~on GaAs! binaries, respectively, are also in good agreement with previous calculations, 7.5 meV per atom[24] and 215.7 meV per atom.[25] The value $\Delta m_b = -0.09$ eV is the point where the bulk composition crosses over from In rich to Ga rich. This point will serve as a reference for assessing surface segregation, below.

C. The 2×2 alloy surface

Next, consider the monolayer cation coverage ~232! surface reconstruction ~Fig. 4!. As shown in Fig. 2, this reconstruction may be stable for laterally compressed InP but unstable for expanded GaP. The ~232! unit cell contains a symmetric, low cation dimer with its atoms in planar sp^2 bonding configurations @with sites labeled l_1 and l_2 in Fig. 4~b!#, and an asymmetric raised dimer with one cation in a medium-low (m) sp^2 configuration and the other in a high (h) pyramidal s^2p^3 configuration. We have previously[12] calculated the energy for $Ga_{1-x}In_xP$ ~232! surfaces containing zero, two, and four In atoms in the four-atom 232 unit cell ~the remainder being Ga!. For surfaces containing two In atoms, we found that a pattern with Ga occupying the l_1 and l_2 sites and In occupying the m and h sites had the lowest energy. This occupation pattern corresponds to bulk $CuPt_B$ ordering. We now expand our earlier calculation to include ~232! surfaces containing one and three surface In atoms per cell. We also allow for In in the second subsurface layer in addition to Ga @on the sites labeled A and B in Fig. 4~b!#. As before, GaAs is used as substrate below the top three atomic layers. For the new surfaces, the minority surface atom can occupy one of the four inequivalent sites in the 232 cell ~l_1, l_2, m, or h!. Based on a spin model[14] fit to our previous results, we expect that an In atom would prefer the medium-low site on the raised dimer (m), and a Ga atom would prefer one of the sites on the low dimer ~l_1 or l_2!. For Ga on the A and B sites, the model fits the present pseudopotential results within 3 meV per surface atom. An outstanding feature of the spin model is strongly dominant on-site interaction terms and almost negligible pair interactions. As we shall see below, this is common to all the surface reconstructions and, to the extent that pair interactions can be completely ignored, causes all ordered surface alloys to have primitive cells equal to that of the associated surface reconstruction.

Figure 4~a! summarizes our results. It shows the calculated relative surface energies for the ~232! surfaces as a function of the chemical potential difference $\Delta m = m_{Ga} - m_{In}$. Each line in the figure is labeled according to the sites occupied by Ga. For instance, *lhm* means that the sites l_1, l_2, h, and m are occupied by Ga and the sites A and B are occupied by In. The lowest-energy surface structures can be grouped into separate regions with transition points indicated by the vertical arrows in Fig. 4~a!. Below $\Delta m = -0.22$ eV, all the surface and subsurface sites are occupied by In. At 20.22 eV, both cations on the low dimer sites change from In to Ga. Between 20.22 eV and 20.07 eV, the low-energy structure

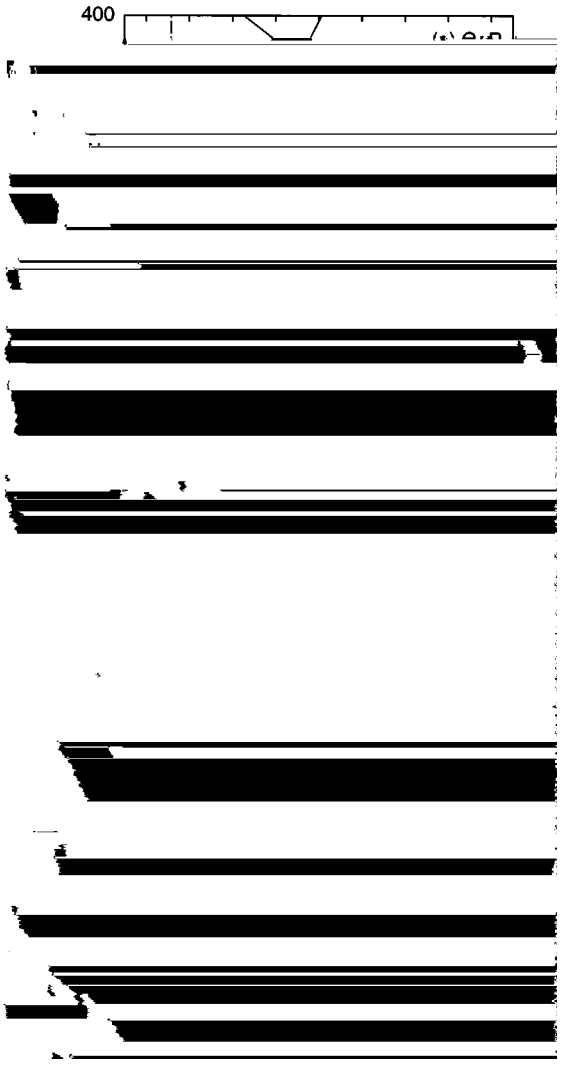

FIG. 2. Relative formation energy per 131 unit cell for ~a! GaP on GaAs, ~b! InP on GaAs, and ~c! GaAs~001! surfaces as a function of the cation chemical potential ~with respect to solid Ga and In!. The dashed vertical lines indicate the limits of the thermodynamically allowed range. The reference composition corresponds to a surface with equal amounts of cations and anions and the zero of energy is chosen for presentation purposes.

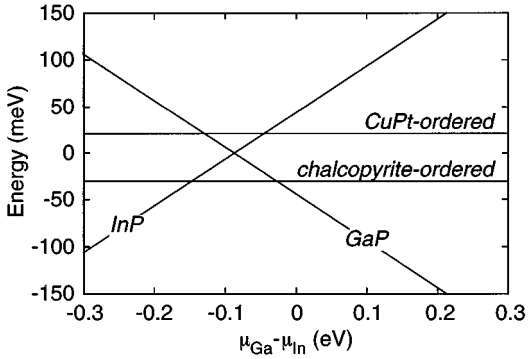

FIG. 3. Relative formation energy per two atoms for bulk GaP, InP, and ordered chalcopyrite-like and CuPt-like $GaInP_2$ as a function of the Ga/In chemical potential difference. The reference composition and the zero of energy are chosen for presentation purposes.

is a $CuPt_B$-ordered $Ga_{0.5}In_{0.5}P$ surface layer with In in the second subsurface layer. At -0.07 and -0.05 eV, the sites in the subsurface layer change their occupation while the surface layer remains CuPt

In the chemical potential range between transitions

At the reference value $\Delta\mu_b = -0.09$ eV, where the bulk composition is $\frac{1}{2}$, only the A sites are occupied by Ga. This gives a layer (In) composition of 6/8. The $c(4\times4)$ surface, therefore, segregates In, although the proximity of the B transition will strongly reduce the segregation at finite temperature.

IV. THE GLOBAL 001 SURFACE STABILITY DIAGRAM

We next combine the results of Figs. 2–7. Because this involves comparing surfaces with different numbers of cations, the Ga and In concentrations are now independent, and a line in a previous figure converts to a surface in the two-dimensional space of $\mu_{Ga}-\mu_{In}$ and $\mu_{Ga}-\mu_{In}$ or, equivalently, μ_{Ga} and μ_{In}. For each pair of chemical potential values, the stable surface configuration is determined by selecting the one with the lowest energy.

A. Surface reconstruction and surface segregation at $T=0$

As discussed previously, for a surface in complete equilibrium with its bulk, μ_P is determined as a function of μ_{Ga} and μ_{In} by the bulk structure with the lowest energy (according to Fig. 3). The result (Fig. 8) is a prediction of the structure and composition (including the occupation pattern) of uppermost four surface layers. (Deeper layers are considered to behave energetically like bulk.) The heavy solid lines in the figure indicate boundaries between different reconstructions. A change in composition without an attendant reconstruction change is indicated by the dashed lines and is labeled according to Figs. 4–7. As expected from our discussion of the binary surfaces (Fig. 2), the cation-terminated (2×2) surface is unstable under Ga-rich conditions with respect to the $b(2\times4)$ surface. However, under more In-rich conditions, the (2×2) CuPt-ordered $GaInP_2$ surface and the InP surface may be stable. Conversely, the cation-terminated $b(2\times4)$ surface

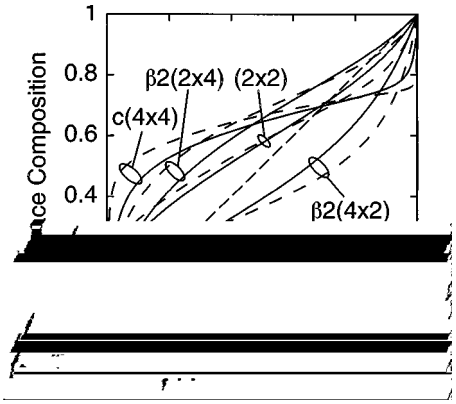

FIG. 9. Surface composition as a function of bulk composition for the $Ga_{1-x}In_xP$~001! surface in the indicated reconstructions at $T=600$ and 900 K. The surface composition is that of the uppermost four layers.

the b2~2×4! surface, and assuming that the growth takes place roughly in the middle of the $GaInP_2$ bulk region ~i.e., at $\Delta\mu=-0.1$ eV!, the energy term $\Delta\mu-\Delta\mu_i$ for site "3" ~see Fig. 6! is −0.1 eV and for site "4" is −0.2 eV. These values are in rough agreement with the values −0.15 to −0.22 eV inferred from the thermodynamic modeling of observed surface segregation at ~001! $Ga_xIn_{1-x}As$ surfaces.[6,9,10] Nagle *et al.*[9] noted that their data for growth on cation-terminated ~4×2! surfaces seemed to indicate a reduced segregation of In, also in accord with our calculation.

We can use the above model to produce quantitative results for segregation at finite temperatures. A comparison of the composition in the top two surface layers with that of the bulk is shown in Fig. 9 for two temperatures, 600 and 900 K. The relationship between the bulk chemical potential and composition was determined using the regular solution model.[31] The energy of the epitaxially constrained random alloy was determined using a linear combination of the bulk structures shown in Fig. 3 with coefficients determined by the tetrahedral cluster probabilities of the random alloy ~$\frac{1}{16}$, $\frac{3}{8}$, $\frac{1}{2}$, and $\frac{1}{16}$ for GaP, chalcopyrite, CuPt, and InP, respectively!.[32] The surface composition is that of the four surface layers shown in Figs. 4–7. Figure 9 confirms our earlier discussions and shows that, in general, the c~4×4! and b2~2×4! segregate In, the b2~4×2! segregates Ga, while the ~2×2! reconstruction is relatively nonsegregating. Not shown in the figure but evident in our calculations is that the surface layer is much more strongly segregating than the subsurface layer. Notice how all the curves in Fig. 9 have derivatives of less than one for intermediate compositions. The composition of the surface, therefore, changes more slowly than that of the bulk. This surface composition pinning is caused by the fact that the chemical potential range over which the surface transforms its composition from In to Ga is much larger than that of the bulk ~compare Figs. 4–7 to Fig. 3!.

Finally, our results suggest a way to create abrupt interfaces in semiconductor heterostructures. If the observed nonabruptness in, e.g., GaAs on InAs growth is caused by interfacial mixing due to In surface segregation, it can perhaps be overcome by changing the chemical potential of both the anion and the cations during growth. The In-rich layers could be grown on the b2~2×4! surface, where In would segregate to the surface, and the Ga-rich layers could be grown on the b2~4×2! surface, where Ga should segregate. The surface segregation effect should then work to make both the In on Ga and the Ga on In interfaces abrupt. Tournie, Trampert, and Ploog[33] have demonstrated that growth on b2~4×2! surfaces is possible, although they were using the reduced anion diffusion rate of the cation-terminated b2~4×2! to increase the critical thickness of strained InAs layers.

C. Surface ordering at $T=0$

Figures 4–7 show that two-dimensional CuPt ordering is possible in the near-surface layers. Figure 3 shows, on the other hand, that chalcopyrite-ordered bulk $GaInP_2$ has a lower energy than that of CuPt-ordered bulk. In order for a surface ordering mechanism to lead to three-dimensional CuPt ordering in thick films, there can, therefore, be no diffusion in the interior of the sample. Such diffusion would destroy the CuPt ordering and lead to chalcopyrite ordering ~at very low T! or a random alloy ~at higher T!. Equilibrium between the bulk and the surface can, therefore, not be present if CuPt ordering is observed. This lack of equilibrium modifies the surface stability diagram. Consider growth where diffusion rates restrict equilibrium to only the top n cation layers. As before, the P chemical potential μ_P is determined according to Eq. ~2! by the bulk composition and structure. The surface structure and composition must, however, remain consistent with the bulk. To see this, imagine changing μ_P slightly so that the crystal grows ~or shrinks!. The nth layer ~before the growth!, which previously was part of the equilibrium, is now out of equilibrium with the surface. Such a situation clearly only makes sense if the nth layer, i.e., the deepest layer in equilibrium with the surface, has the composition and structure of the bulk. In the calculation of the stability diagram, we must therefore only include structures whose occupation patterns in layer n and below are like bulk. Motivated by experiment, we consider the bulk structures GaP, InP, and CuPt-ordered $GaInP_2$. For each of these bulk structures, a surface stability diagram is computed, and the stability region of the surface whose nth cation layer composition and structure is consistent with ~same as! the bulk is extracted and shown in Fig. 10 for $n=1$ and Fig. 11 for $n=2$ @$n=1$ for the c~4×4! surface#. Thus, Figs. 10 and 11 represent stability diagrams for surfaces where diffusion is limited to the top two and the top four monolayers, respectively. The gross features of the resulting stability diagram resembles Fig. 8 with some minor shifts of boundaries. Some regions overlap slightly, indicating hysteresis, and gaps are seen where no surface structure consistent with the three bulk structures was found. Regions of CuPt-ordered $GaInP_2$ exist in Fig. 10 for the ~2×2! reconstruction and in Fig. 11 for the b2~2×4! and the c~4×4! surfaces, with the latter being A type. For the b2~4×2! surface, as discussed in Section III D, perfect CuPt ordering does not exist.

D. Surface ordering at finite T

We can use the thermodynamic model discussed in Section IV B, above, to calculate the occupation or composition of each site as a function of temperature. For each surface reconstruction, we focus on the layer that shows the strongest tendency to order. This includes the surface layer for the

~2 3 2! surface, the second subsurface layer for the *b*2~4 3 2! and the *c*~4 3 4! surfaces, and the third subsurface layer for the *b*2~2 3 4! surface. The chemical potential $\Delta\mu = \mu_{Ga} - \mu_{In}$ is calculated as a function of T by requiring that the average composition is $\frac{1}{2}$. $CuPt_B$ and $CuPt_A$ order parameters are calculated from the appropriate site composition differences. The results are shown in Fig. 12. The surfaces with the strongest tendency for ordering are the $CuPt_B$-ordered ~2 3 2! surface @Fig. 12~a!# and the $CuPt_A$-ordered *c*~4 3 4! surface @Fig. 12~d!#. The current ~2 3 2! results are identical to our previous results shown in Fig. 6~b! in Ref. 14. As discussed in Sec. III D, our choice of layer composition causes the *b*2~4 3 2! surface @Fig. 12~b!# to order weakly in the second subsurface layer with nonzero order parameters for both $CuPt_A$ and $CuPt_B$ ordering. The *b*2~2 3 4! surface @Fig. 12~c!# is relatively strongly $CuPt_B$ ordered. The *b*2~2 3 4! surface has only half the number of ordering-inducing top-layer dimers as that of the surface used in our earlier calculation @see Fig. 8~b! in Ref. 14#, where a much larger degree of order was observed. Obviously, low diffusion rates combined

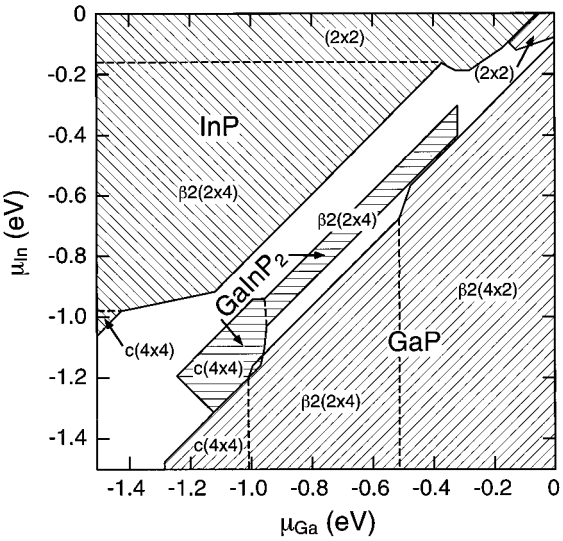

FIG. 11. $T = 0$ surface stability diagram of the Ga

with high growth rates will reduce the degree of order that is achieved in the subsurface layers. The observed degree of order for the $c(4\times4)$ and $b(2\times2)$ surfaces may therefore be much less than predicted in Figs. 12(c) and 12(d).